Interaction of DNA with Cationic Micelles: Effects of Micelle Surface Charge Density, Micelle Shape, and Ionic Strength on Complexation and DNA Collapse

Yilin Wang, Paul L. Dubin,* and Huiwen Zhang†

Department of Chemistry, Indiana University-Purdue University, Indianapolis, Indiana 46202

Received July 27, 2000. In Final Form: November 29, 2000

Complexation between DNA and cationic/nonionic micelles of dodecyldimethylamine oxide (DMDAO) at various ionic strengths (I) was studied by monitoring turbidity or dynamic light scattering as a function of pH at various ionic strengths (I). Complexation takes place at a critical degree of micelle protonation (β_c) and is therefore primarily controlled by the ratio of cationic:nonionic surfactant, not by the ratio of surfactant:DNA. β_c corresponds to a critical micelle surface charge density (σ_c), which increases nearly linearly with I. The dependence of β_c on I displays a discontinuity when the DMDAO micelle shape changes from spherical to rodlike. The proximity of the complexation boundary to the coil/coil−globule coexistence boundary reported from fluorescence microscopy[1] indicates that the DNA−micelle complexation observed by scattering also corresponds to micelle-induced collapse of DNA.

Introduction

Studies of complex formation between DNA and a cationic amphiphilic molecule have implications for gene therapy,[2] a conceptually new approach for the treatment of human disease,[3−7] which is rapidly progressing from basic research and toward clinical application.[8,9] One limiting factor for gene therapy is DNA transport, since, under normal physiological conditions, DNA is a large highly charged particle that is repelled by the similarly negative cell membrane. Charge neutralization is the basis for the potency of cationic lipid transfer agents,[5,10−13] and several synthetic cationic lipids and cationic liposome formulations are commercially available.[10,14−16] After the first demonstration of cationic lipid-mediated gene delivery by Felgner and colleagues[10] two decades ago, considerable progress has been made in transfection efficiency.[11,17] However, at present, no single lipid fulfills the criteria for an efficient and harmless vector for gene delivery.

Most of the factors affecting the efficiency of DNA delivery are related to the physicochemical properties of the DNA−lipid complex, including its structure,[18,19] morphology,[20−23] surface charge,[15,19,24] and solubility.[6] DNA delivery appears to be most efficient when complexes are formed at a ratio of lipid positive charges to DNA negative charges of about 1 or more,[15,24] presumably because positively charged complexes are attracted to the cell surface. However, nearly neutral complexes tend to aggregate in aqueous solution and exhibit condensed structures,[20−23] typically leading to the formation of large aggregates, whose limited solubility may result in poor diffusion within tissues, and even trapping in blood vessels.[25,26] In addition to lipid:DNA stoichiometry, environmental parameters, such as ionic strength and pH, can affect DNA delivery. However, the relationships among these physicochemical properties have not yet been clarified.

In the present work, we study complexation of DNA with a simple model amphiphile, dodecyldimethylamine oxide (DMDAO). DMDAO can exist in either nonionic or cationic (protonated) form,[27−30] which results in a pH-

* To whom correspondence should be addressed.
† Current address: SLTP Co. Ltd., 588 Jiu Xing Rd., Shanghai 20614, PRC.

(1) Mel'nikova, Y. S.; Lindman, B. *Langmuir* **2000**, *16*, 5871−5878.
(2) Lasic, D. D. *Liposomes in Gene Delivery*; CRC Press: Boca Raton, FL, 1997.
(3) Mulligan, R. C. *Science* **1993**, *260*, 926−932.
(4) Rädler, J. O.; Koltover, I.; Salditt, T.; Safinya, C. R. *Science* **1997**, *275*, 810−814.
(5) Miller, A. D. *Angew. Chem., Int. Ed. Engl.* **1998**, *37*, 1768−1785.
(6) Huang, L., Hung, M. C., Wagner, E., Eds.; *Nonviral Vectors for Gene Therapy*; Academic Press: New York, 1999.
(7) Kozarsky, K. F.; Wilson, J. M. *Curr. Opin. Genetic Dev.* **1993**, *3*, 499−503.
(8) Verma, I. M.; Somia, N. *Nature* **1997**, *389*, 239−242.
(9) Anderson, W. F. *Nature* **1998**, *392*, 25−30.
(10) Felgner, P. L.; Gadek, T. R.; Holm, M.; Roman, R.; Chan, H. W.; Wenz, M.; Northrop, J. P.; Ringold, G. M.; Danielsen, M. *Proc. Natl. Acad. Sci. U.S.A.* **1987**, *84*, 7413−7417.
(11) Gao, X.; Huang, L. *Gene Ther.* **1995**, *2*, 710−722.
(12) Ren, T.; Zhang, G. S.; Song, Y. K.; Liu, D. *J. Drug Targeting* **1999**, *7*, 285−292.
(13) Ren, T.; Young, K. S.; Zhang, G.; Liu, D. *Gene Ther.* **2000**, *7*, 764−768.
(14) Leventis, R.; Silvius, J. R. *Biochim. Biophys. Acta* **1990**, *1023*, 124−132.
(15) Behr, J.-P.; Demeneix, B.; Loeffler, J.-P.; Perez-Mutul, J. *Proc. Natl. Acad. Sci. U.S.A.* **1989**, *86*, 6982−6986.
(16) Kunitake, T.; Okahata, Y.; Tamaki, K.; Kumamaru, F.; Takayanagi, M. *Chem. Lett.* **1977**, 387−390.
(17) Felgner, P. L. *Hum. Gene Ther.* **1996**, *7*, 1791−1793.
(18) Sternberg, B.; Sorgi, F. L.; Huang, L. *FEBS Lett.* **1994**, *356*, 361−366.
(19) Gershon, H.; Ghirlando, R.; Guttman, S. B.; Minsky, A. *Biochemistry* **1993**, *32*, 7143−7151.
(20) Mel'nikov, Y. S.; Sergeyev, V. G.; Yoshikawa, K. *J. Am. Chem. Soc.* **1995**, *117*, 2401−2408.
(21) Mel'nikov, Y. S.; Sergeyev, V. G.; Yoshikawa, K. *J. Am. Chem. Soc.* **1995**, *117*, 9951−9956.
(22) Mel'nikov, Y. S.; Sergeyev, V. G.; Yoshikawa, K.; Takahashi, H.; Hatta, I. *J. Chem. Phys.* **1997**, *107*, 6917−6924.
(23) Spink, C. H.; Chaires, J. B. *J. Am. Chem. Soc.* **1997**, *119*, 10920−10928.
(24) Schwartz, B.; Benoist, C.; Abdallah, B.; Scherman, D.; Behr, J.-P.; Demeneix, B. A. *Hum. Gene Ther.* **1995**, *6*, 1515−1524.
(25) Allen, T. M.; Stuart, D. D. In *Liposome, Rational Design*; Janaff, A. S., Ed.; Marcel Dekker: New York, 1999; pp 63−87.
(26) Li, S.; Huang, L. In *Liposome, Rational Design*; Janaff, A. S., Ed.; Marcel Dekker: New York, 1999; pp 89−124.
(27) Ikeda, S.; Tsunoda, M.; Maeda, H. *J. Colloid Interface Sci.* **1978**, *67*, 336−348.
(28) Ikeda, S.; Tsunoda, M.; Maeda, H. *J. Colloid Interface Sci.* **1979**, *70*, 448−455.
(29) Imaishi, Y.; Kakehashi, R.; Nezu, T.; Maeda, H. *J. Colloid Interface Sci.* **1998**, *197*, 309−316.
(30) Maeda, H.; Muroi, S.; Kakehashi, R. *J. Phys. Chem. B* **1997**, *101*, 7378−7382.

10.1021/la0010673 CCC: $20.00
Published on Web 02/01/2001

dependent variation of DMDAO micelle surface charge density. Since both the degree of protonation (β) and ionic strength (I) affect the micelle shape and size,[31,32] the DNA−DMDAO system facilitates a systematic study of the effects of micelle charge density, micelle shape, and ionic strength on DNA−amphiphile complexation. Recently, Mel'nikova and Lindman[1] studied the behavior of this system as a function of pH and I using fluorescence microscopy. A collapse from coil to globule was observed at certain combinations of pH and I. Our previous studies on the binding of DMDAO with PAMPS,[33] P(AMPS−NVP),[33] and NaPSS[31,34] indicated that complex formation between DMDAO micelles and polyelectrolytes occurs at a critical pH, corresponding to a critical β, i.e., corresponding to a critical micelle surface charge density σ. The critical σ was observed to depend in a rather simple way on I. These above studies encouraged us to obtain a better understanding on the relationship between polyelectrolyte−micelle complexation and the collapse of DNA in the presence of micelles. Here, we focus our efforts on whether "complexation" and collapse are the same phenomenon by comparing the present work with microscopic observations and in so doing observe a correlation between the I dependence of β_c and the micelle shape.

Experimental Section

Materials. DNA from salmon testes with average molecular weight of 2×10^6 was purchased from Sigma and *N*,*N*-dimethyldodecylamine oxide (DMDAO, purity >98%) from Fluka. HCl standard solution and NaCl were obtained from Fisher. All were used without further purification. Distilled water was used in all experiments.

Turbidimetric Titrations. Turbidimetric titrations were carried out at 25 ± 1 °C by adding 0.200 M HCl standard solution to solutions of 0.100 g/L DNA and 1, 2, 10, or 50 mM DMDAO at fixed ionic strengths and monitoring pH and turbidity simultaneously. pH measurements were made under N_2 with a Corning pH meter240 equipped with a Beckmann combination electrode. Turbidity measurements, reported as $100 - \%T$, were performed at 420 nm using a Brinkman PC800 probe colorimeter equipped with a 1 cm path length fiber-optics probe. Measured turbidity values were corrected by subtracting the turbidity of a DNA-free blank. pH and turbidity values were recorded when the meter responses were constant for 2 min. The time required to reach this equilibrium varied from 2 min for clear solutions to ca. 2−10 min for more turbid samples.

Dynamic Light Scattering (QELS). All measurements were carried out at a scattering angle of 90° and at 25.0 ± 0.5 °C with a DynaPro-801 (Protein Solutions Inc., Charlottesville, VA), which employs a 30 mW solid-state 780 nm laser and an avalanche photodiode detector. Samples with 50 mM DMDAO at desired pH and ionic strength were prepared and introduced into the 7 μL cell through a 0.20 μm filter prior to measurement. The correlation function of the scattering data was analyzed via the method of regularization[35] and then used to determine the diffusion coefficient D of the solutes. The diffusion coefficient D can be converted into the apparent equivalent hydrodynamic radius R_h using the Stokes−Einstein equation for a sphere

$$R_h = \frac{kT}{6\pi\eta D} \tag{1}$$

where k is the Boltzmann constant, T is the absolute temperature, and η is the solvent viscosity. However, for rodlike micelles we use the Perrin relationship[36−38] for the translational diffusion coefficient of ellipsoidal molecules:

$$D = \frac{kT}{6\pi\eta a} G(\rho) \tag{2}$$

where $G(\rho)$ has the form

$$G(\rho) = (1 - \rho^2)^{-1/2} \ln\left\{\frac{1 + (1 - \rho^2)^{1/2}}{\rho}\right\} \qquad \rho < 1 \tag{3}$$

where ρ is the axial ratio, $\rho \equiv b/a$, and a and b are the major semiaxis and minor semiaxis, respectively. We assume that b is equal to the radius of largest spherical micelle, which is taken as the micelle radius above which bimodal distribution of micelles are observed.[31,32] The diffusion coefficients of micelles were fitted to eqs 2 and 3 to determine the shape of DMDAO micelles. When a is equal to b, the micelle is spherical; when a is larger than b, the micelle is rodlike.

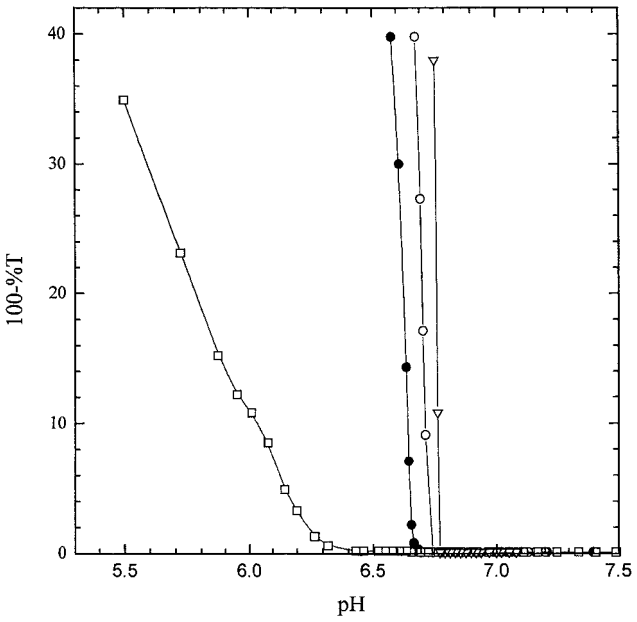

Figure 1. Turbidimetric titration of 0.100 g/L DNA and 1, 2, 10, or 50 mM DMDAO in 0.10 M NaCl with 0.200 M HCl: (□) 1 mM; (●) 2 mM; (○) 10 mM; (▽) 50 mM.

Results and Discussion

Turbidimetric titration curves of DNA−DMDAO at 0.10 M NaCl obtained upon decreasing pH are shown in Figure 1. The turbidity, which is constant and very small at high pH values, displays a well-defined increase at pH_c, corresponding to the binding of DNA with DMDAO. pH_c is almost independent of DMDAO concentration in the range 2−50 mM, and the shapes of titration curves are almost the same despite the large DMDAO concentration range; however, for 1 mM DMDAO, pH_c deviates sharply, as does the shape of the curve. Since the critical micelle concentration (cmc) of DMDAO at $I = 0.10$ is about 1.3 mM,[30] this result is best explained by concluding that DMDAO binds to DNA as monomer surfactant molecules below cmc but as micelles above cmc. The pH at which DMDAO micelles begin to bind to DNA, as detected by the onset of turbidity, is defined as the point of incipient complex formation. Complexation leads to a dramatic increase in turbidity, because the average molecular mass

(31) Dubin, P. L.; Chew, C. H.; Gan, L. M. *J. Colloid Interface Sci.* **1989**, *128*, 566−576.
(32) Zhang, H.; Dubin, P. L.; Kaplan, J. I. *Langmuir* **1991**, *7*, 2103−2107.
(33) Dubin, P. L.; Thé, S. S.; McQuigg, D. W.; Chew, C. H.; Gan, L. M. *Langmuir* **1989**, *5*, 89−95.
(34) McQuigg, D. W.; Kaplan, J. I.; Dubin, P. L. *J. Phys. Chem.* **1992**, *96*, 1973−1978.
(35) Provencher, S. W. *Comput. Phys. Commun.* **1982**, *27*, 229.
(36) Perrin, F. *J. Phys. Radium* **1934**, *V*, 497.
(37) Perrin, F. *J. Phys. Radium* **1936**, *VII*, 1.
(38) Berne, B. J.; Pecora, R. In *Dynamic Light Scattering with Applications to Chemistry, Biology, and Physics*; John Wiley & Sons: New York, 1976; p 143.

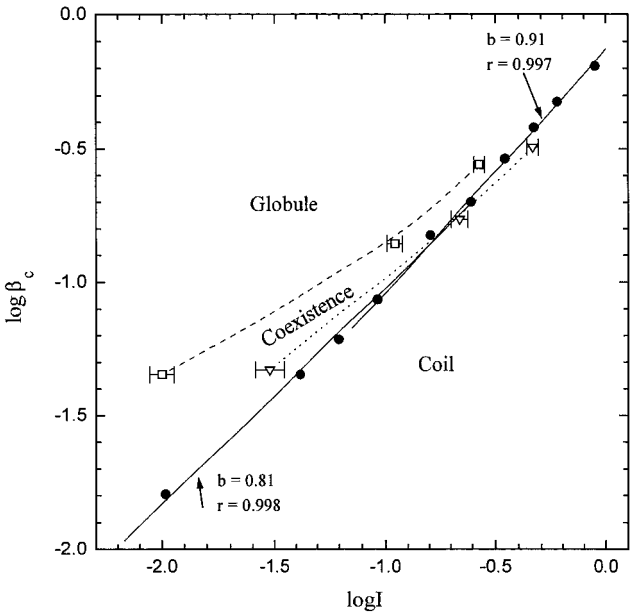

Figure 2. Dependence of the critical protonation degree of DMDAO micelle on ionic strength for the DMDAO−DNA system. *b* and *r* are slope and correlation coefficient, respectively. Phase boundary for complexation from this work (●). Dotted line (▽) indicates β values at which DNA collapsed state is first observed; dashed line (□) indicates β values at which DNA coiled states are no longer observed (both converted from the phase boundaries expressed by pH and *I* in ref 1).

of DNA−DMDAO complexes is much larger than for DNA alone, as observed in polycation−micelle complexes[39] and in polyanion−DMDAO complexes,[31,33] in which systems the critical pH is verified by dynamic light scattering, electrophoretic light scattering, and other techniques. It is important to point out the ratio of total cationic surfactant to DNA can change by a factor of 25 with very little effect on the critical pH. This shows that the strength of binding is controlled by the micelle surface charge density and not by the stoichiometry: if β is not large enough, DNA will not bind DMDAO no matter how much surfactant is added.

Since we work at [DMDAO]/cmc ≫ 50 in the following experiments, the molar concentration of monomer surfactant can be ignored. Then, the effective logarithmic ionization constant pK_b of the protonation equilibrium of the micellar solution[40] is

$$pK_\beta = pH + \log[\beta(1-\beta)^{-1}] \quad (4)$$

Here, β is the degree of protonation of micellar DMDAO, and pK_β depends on ionic strength. pK_β is a function of β, and β decreases with an increase of pH. DMDAO forms nonionic micelles at pH > 9, cationic micelles at pH < 3, and cationic−nonionic mixed micelles at intermediate pH.[41]

Turbidimetric titrations of 1 g/L DNA and 50 mM DMDAO were carried out at various ionic strengths. pH_c values were converted to β_c which corresponds to a critical micelle surface charge density using pH titration curves obtained at various ionic strengths for 50 mM DMDAO.[32] The critical conditions for complexation of DNA with DMDAO micelles are then described by the phase boundary demonstrated in Figure 2.

The formation of DNA−amphiphile complexes normally induces a conformational change in DNA.[20−22] Recently, Mel'nikova and Lindman[1] studied the conformational behavior of DNA in the presence of DMDAO micelles using fluorescence microscopy as a function of ionic strength and pH. They identified three states: coil, globule, and coil−globule coexistence. The corresponding phase boundaries are compared in Figure 2 with the phase boundary in the present work. The proximity of β_c to the coil/coexistence boundary shows that complexation detected turbidimetrically occurs along with the collapse transition. The driving force for the transition from coil to globule should be incompatibility with solvent.[20] Complexation between DNA and DMDAO must be accompanied by charge neutralization and loss of DNA counterions, i.e., the same phenomenon as DNA collapse induced by the binding of polycations.[42,43]

The phase boundary in Figure 2 arises from the screening by salt of electrostatic interactions between DNA and micelles, which decreases the binding affinity of micelles to DNA, thus requiring an increase of micelle surface charge density for complexation. Theory and experiment indicate that the critical colloid surface charge density for polyelectrolyte−colloid binding may be expressed as[31,44−46]

$$\sigma_c\xi \propto \kappa^a = cI^{a/2} \quad (5)$$

where σ_c is the critical colloid surface charge density, ξ is linear charge density of the polyelectrolyte (here DNA), κ is the Debye−Hückel parameter, and *c* and *a* are constants. In previous work,[31,33,34] the micelle electrostatic surface potential ψ_0 was first obtained from β_c by calculating from the difference between the effective pK_β and intrinsic value pK_0 (pK_β at $\beta \to 0$),[32,47]

$$pK_\beta - pK_0 = -0.434(e\psi_0/kT) \quad (6)$$

where *k* and *T* are the Boltzmann constant and the temperature, respectively. Then, σ_c was deduced from ψ_0 by application of the Gouy−Chapman equation[48] for a sphere of radius *a*,

$$\sigma_c = (\epsilon\psi_0/4\pi)(\kappa + 1/a) \quad (7)$$

where ϵ is the solvent dielectric constant. However, as pointed out by Mille[49] and as noted by us, this analysis assumed that the micelles were spherical and also ignored hydrogen bonding between polar headgroups of DMDAO molecules in micelles. The exact calculation of σ_c from β_c is thus complicated. However, since β_c is proportional to σ_c,[31] a plot of log β_c vs log *I* should, according to eq 5, be linear.

As seen in Figure 2, the slopes and correlation coefficients of the log β_c−log *I* lines are $b = 0.81$ and $r = 0.998$ for $I < 0.20$ and $b = 0.91$ and $r = 0.997$ for $I > 0.20$,

(39) Xia, J.; Zhang, H.; Rigsbee, D. R.; Dubin, P. L.; Shaikh, T. *Macromolecules* **1993**, *26*, 2759−2766.
(40) Imae, T.; Konishi, H.; Ikeda, S. *J. Phys. Chem.* **1986**, *90*, 1417−1422.
(41) Herrmann, K. W. *J. Phys. Chem.* **1964**, *68*, 1540−1546.
(42) Takahashi, M.; Yoshikawa, K.; Vasilevskaya, V. V.; Khokhlov, A. R. *J. Phys. Chem. B* **1997**, *101*, 9396−9401.
(43) Chen, W.; Turro, N. J.; Tomalia, D. A. *Langmuir* **2000**, *16*, 15−19.
(44) Muthukumar, M. *J. Chem. Phys.* **1987**, *86*, 7230−7235.
(45) von Goeler, F.; Muthukumar, M. *J. Chem. Phys.* **1994**, *100*, 7796−7803.
(46) Zhang, H.; Dubin, P. L.; Ray, J.; Manning, G. S.; Moorefield, C. N.; Newkome, G. R. *J. Phys. Chem. B* **1999**, *103*, 2347−2354.
(47) Tokiwa, F. *Adv. Colloid Interface Sci.* **1972**, *3*, 389.
(48) Hiemenz, P. C. In *Principles of Colloid and Surface Chemistry*; Marcel Dekker: New York, 1977; Chapter 9.
(49) Mille, M. *J. Colloid Interface Sci.* **1981**, *81*, 169−179.

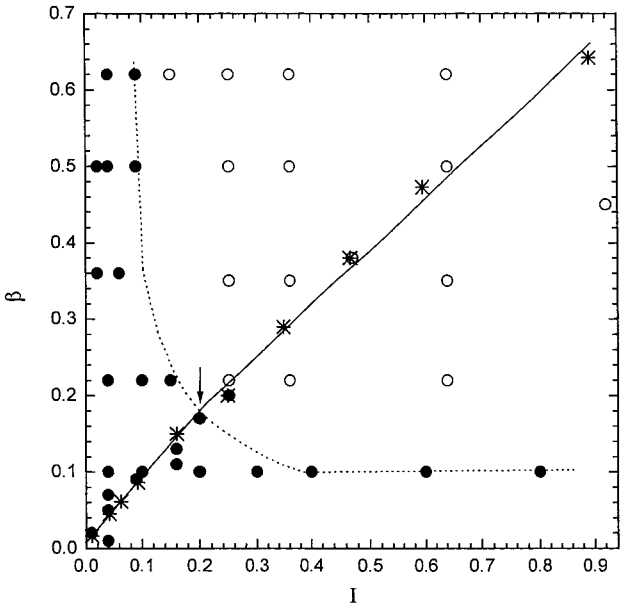

Figure 3. Distribution of DMDAO micelle shape at 50 mM and at different ionic strength (I) and different protonation degree (β) summarized from dyamic light scattering measurement: (○) rod; (●) sphere; (*) DNA−DMDAO phase boundary; the arrow corresponds to the slope change in Figure 2.

respectively. The remarkable quality of the fits, as expressed by correlation coefficients extremely close to unity, enables us to assert that log β_c vs log I indeed displays a discontinuity at $I \approx 0.20$ M and $\beta_c \approx 0.20$. DMDAO micelle shapes determined by dynamic light scattering as a function of β and I are summarized in Figure 3. The phase boundary for DNA−DMDAO complexation (solid line) goes through the sphere−rod transition for DNA-free DMDAO at $I \approx 0.2$ and $\beta \approx 0.17$, which coincides with the break in the phase boundary in Figure 2, indicating that the discontinuity in the phase boundary takes place at the sphere−rod transition of DMDAO micelles. This may be explained in two ways. The first explanation is that at conditions of β and I corresponding to spherical micelles the large micelle curvature could reduce the interaction contact area between micelles and the stiff DNA chain. Second, the dependence of micelle surface potential on β differs for spheres and rods,[31] so that conversion of the curve of Figure 2 to σ_c from β_c could either diminish or amplify the change in slope. Resolution between these alternative hypotheses may be possible, but since the main goal of the present paper is the comparison of complexation with collapse, a more quantitative physical analysis of the effects of micelle shape, size, and surface charge density, as well as polymer persistence length, will be presented elsewhere.

Conclusions

The binding of DNA to DMDAO at surfactant concentration above cmc is dominated by simple electrostatics and therefore primarily controlled by micelle surface charge density and the ionic strength. Complexation occurs at a critical micelle surface charge density, which increases nearly linearly with ionic strength. This critical micelle surface charge density shows little if any dependence on micelle concentration, so that charge equivalency (DNA−amphiphile stoichiometry) does not control binding. A secondary effect is related to the micelle shape, as evidenced by a small but significant change in the ionic strength dependence of the critical micelle surface charge density when the micelle dimension change from spherical to rodlike. Comparison with fluorescence microscopy data reported elsewhere[1] reveals that the critical binding point corresponds to micelle-induced collapse of DNA.

Acknowledgment. This work was supported by NSF (DMR-0076068).

LA0010673